A pulsed source for Xe(6s[3/2]1) and Xe(6s′[1/2]1) resonance state atoms using two photon driven amplified spontaneous emission from the Xe(6p) and Xe(6p′) states

V. A. Alekseev and D. W. Setser

Citation: The Journal of Chemical Physics **105**, 4613 (1996); doi: 10.1063/1.472304
View online: http://dx.doi.org/10.1063/1.472304
View Table of Contents: http://scitation.aip.org/content/aip/journal/jcp/105/11?ver=pdfcov
Published by the AIP Publishing

A pulsed source for Xe($6s[3/2]_1$) and Xe($6s'[1/2]_1$) resonance state atoms using two-photon driven amplified spontaneous emission from the Xe($6p$) and Xe($6p'$) states

V. A. Alekseev[a] and D. W. Setser
Department of Chemistry, Kansas State University, Manhattan, Kansas 66506

(Received 18 April 1996; accepted 10 June 1996)

A new, simple method for the generation of Xe($6s[3/2]_1$) and Xe($6s'[1/2]_1$) atoms is described. The method involves resonant two-photon excitation of Xe($6p[1/2]_0$ and $6p'[3/2]_2$) states followed by amplified spontaneous emission (ASE) to the Xe($6s[3/2]_1$ and $6s'[1/2]_1$) states. The vacuum ultraviolet transitions, Xe($6s[3/2]_1 \rightarrow 5p^6(^1S_0)$) at 147 nm and Xe($6s'[1/2]_1 \rightarrow 5p^6(^1S_0)$) at 129.6 nm, were used to monitor the time dependence of the resonance state atom concentrations. The quenching rate constants of these resonance atoms with ten molecules were measured at 300 K. The quenching cross-sections of the Xe($6s$ and $6s'$) resonance atoms are compared to the cross-sections of the metastable Xe($6s[3/2]_2$) atoms and Xe($6p[3/2]_2$) atoms. The correlation between quenching cross-sections and photoabsorption cross-section of the molecules predicted by the resonance dipole–dipole energy transfer model is discussed. The applicability of the two-photon driven ASE method for the generation of other resonance state atoms is considered. © *1996 American Institute of Physics.* [S0021-9606(96)00335-2]

I. INTRODUCTION

The collisional deactivation of excited rare gas atoms by molecules is an important aspect of both fundamental and applied chemical physics. Reactions of the $(n+1s,np^5)J=0,2$ metastable states of the rare gas atoms have been studied in a systematic way for a wide group of molecules.[1–3] Unlike the metastable states, experimental data for the $(n+1,np^5)J=1$, resonance state rare gas atoms is not very extensive. The major share of the data for the resonance states is for the lighter atoms, He[4], Ne[5], and Ar[6]; the data for Kr[7] and Xe[8] are limited and mainly have been obtained using the steady-state sensitization method. Yu measured relative quenching rate constants of the lowest energy Xe($6s[3/2]_1$) resonance state (67,068 cm^{-1}) atoms with 21 molecules using this method.[8(b)] To the best of our knowledge, no attempts have been made to study systematically the deactivation of the second Xe($6s'[1/2]_1$) resonance state (77,186 cm^{-1}) by molecular reagents. However, two- and three-body removal processes of the resonance atoms in xenon and other rare gases have been studied.[9]

Comparison of quenching rate constants for the resonance and metastable atoms is of interest for understanding differences in the deactivation mechanisms of spin–orbit states of nearly the same energy with a given electron configuration. The dipole–dipole energy transfer model is one mechanism for deactivation of the resonance states. This model, as developed by Watanabe and Katsuura,[10] predicts a correlation between the quenching cross-sections and the photoabsorption cross-sections of reagent molecules at the wavelength of the resonance atomic emission. This model seems to show agreement with the experimental quenching cross-sections for the resonance states of He and Ar.[4,5,6(b),6(c),11] The quenching cross-sections of the metastable and resonance states of heavier rare gases are of similar magnitude,[6] but the dipole–dipole mechanism cannot apply to the metastable states. The deactivation mechanism for the latter is usually formulated as a coupling of the entrance channel potential to a large number of exit channels potentials with a probability, P, for excitation-transfer for those trajectories passing the orbiting distance.[1(b)] Comparison of the quenching cross-sections of the resonance and metastable Xe($6s,6s'$) states will be useful for further elucidation of the quenching mechanisms, because the lower energy of the Xe($6s,6s'$) atoms reduces the number of exit channels, which makes experimental tests easier to design. The reactive quenching of Xe($6s[3/2]_1$) atoms by halogen-containing molecules (RX) closely resembles the metastable atom reactions.[7,8] If the dipole–dipole mechanism is operative for Xe($6s[3/2]_1$) atoms interacting with RX molecules, it must be in competition with the covalent-ionic curve-crossing mechanism.

The main difficulty for experiments with Xe resonance state atoms has been the lack of a good method for preparation. Tunable lasers in the vacuum ultraviolet range are not available, two-photon excitation from the ground state is prohibited by selection rules, and three-photon excitation is inefficient. Pulsed discharges and electron beams do not provide selective excitation and, in addition, experimental artifacts related to the presence of thermal electrons, ions, and decomposition of the molecular reagent can seriously influence the kinetic data.

Resonant, single-color, two-photon excitation of Xe($6p$ and $6p'$) states gives amplified spontaneous emission (ASE) to lower lying states, including the $6s'[1/2]_1$ and $6s[3/2]_1$ resonance states; see Fig. 1.[12] The intensity of the ASE is strong for laser energies >0.1 mJ and the width of ASE

[a]Permanent address: Photonics Department, Institute of Physics, St. Petersburg University, 198904 St. Petersburg, Russia.

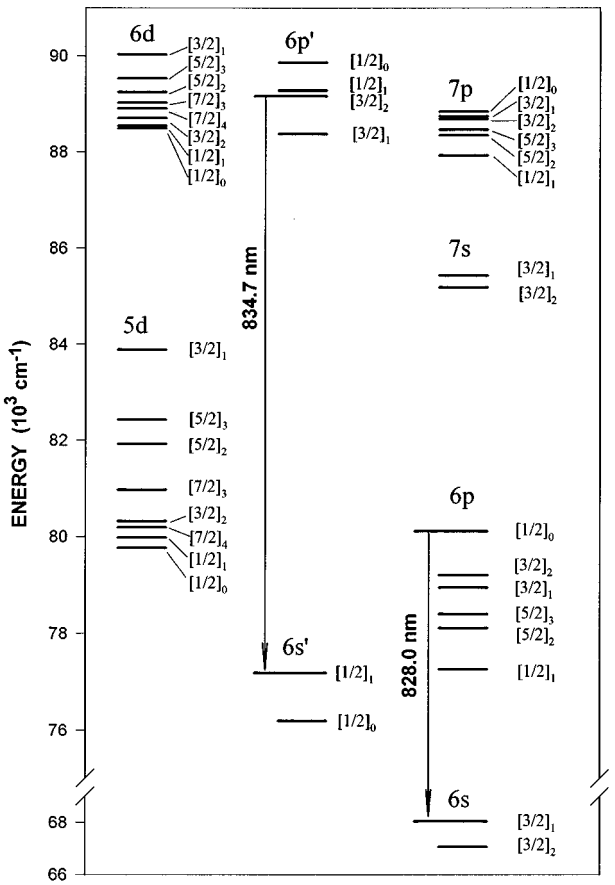

FIG. 1. Energy level diagram for states of Xe. The states are identified using the Racah notation. The ASE transitions used for generation of the resonance state atoms are shown.

pulse is similar to, or even less, than the width of the laser pulse. Due to the strong interaction of the excited atoms with the laser and self-generated emissions, the laser-prepared state is almost completely depopulated by the end of laser pulse.[12] The purpose of the present paper is to show that two-photon excitation of Xe($6p$,$6p'$) states followed by ASE can be used as a simple and efficient method for the generation of $6s[3/2]_1$ and $6s'[1/2]_1$ resonance state atoms on a 15 ns time scale in an environment suitable for kinetic studies. In addition to true ASE, two-photon interaction with the Xe($6p$,$6p'$) states can generate other nonlinear processes. We will collectively refer to all of these processes as ASE, unless a need exists to make a distinction among them. In the remainder of the text, Xe usually will be omitted from the atomic term description.

II. EXPERIMENTAL METHODS

A diagram of the experimental apparatus is shown in Fig. 2. The output from a Lambda Physik dye laser (LPD 3002) pumped with a XeCl laser (Questek 2840) was doubled with BBO-I crystal to provide tunable ultraviolet laser pulses. Coumarin 440 and 503 dyes were used to obtain 225 and 250 nm for two-photon excitation of Xe($6p'$) and Xe($6p$) states, respectively. The laser pulse had a full-width

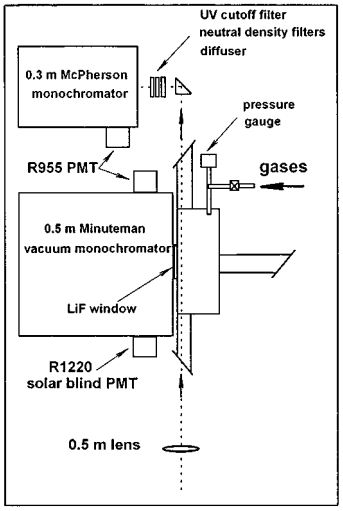

FIG. 2. Schematic diagram of the experimental apparatus. The optical pathway of the laser beam is shown by the dotted line. The nominal distance between the laser beam and LiF window separating the cell from the monochromator is ~1 mm.

at half-maximum of ~15 ns and the energy was 0.1–0.4 mJ per pulse, as measured with a Precision power meter (Model RJP-735). The dye laser was operated without an etalon and the band width was 22 GHz for the doubled wavelength. The experiments were performed in a stainless steel cell with 25 cm long baffle arms. The cell, which was attached to the entrance flange of a monochromator (0.5 Minuteman), had a LiF window for observation of the vacuum ultraviolet (vac. UV) emission. The laser beam, which passed vertically through the cell, was parallel to the entrance slit of the monochromator. The laser beam was directed to within 2–3 mm of the LiF window. Most experiments were done with mildly focused conditions using a 50 cm focal length lens.

The monochromator was equipped with a 1200 g/mm grating blazed at 120 nm and Hamamatsu R1220 solar blind photomultiplier tube (PMT), which has maximum sensitivity at ~200 nm, but the range extends to 115 nm. The visible emission was observed using a 1200 g/mm grating blazed at 500 nm and a Hamamatsu R955 photomultiplier tube. The output signal of the PMT was digitized (Hewlett-Packard 54510 A digital storage oscilloscope) and transferred to a computer for storage and analysis. To prevent absorption of 129.6 nm emission, the monochromator was evacuated using a mechanical pump in combination with a diffusion pump. The pressure in the monochromator was less then 10^{-4} Torr. Experiments in which the 147 nm emission from Xe($6s[3/2]_1$) atoms was measured were performed by flushing the monochromator with nitrogen or by evacuation, as described above.

The Xe($6p \rightarrow 6s$) and Xe($6p' \rightarrow 6s$,$6s'$) ASE emission in the forward direction was monitored with a 0.3 m McPherson monochromator equipped with R955 Hamamatsu PMT. After passing through the cell, the laser beam and associated ASE were directed to the entrance slit of this monochromator; a filter was used to cut the UV laser light. The intensity of the ASE lines was extremely strong, and a

combination of neutral density filters with a diffuser (an etched quartz plate) were placed in front of the entrance slit to fill the monochromator optics with light and to avoid damage of the PMT. The Xe emission was also observed in the backward direction relative to propagation of the laser beam. A quartz plate, placed near the entrance window of the cell with a 45° angle to the laser beam, was used to direct the backward ASE to the entrance slit of the 0.3 m monochromator.

When the Xe($6p'$ and $6p$) states were excited with laser pulses of a similar energy, the ASE signals originating from transitions to the $6s'[1/2]_1$ and $6s[3/2]_1$ states were of comparable intensity. However, the sensitivity of our vac. UV registration system drops dramatically in the short wavelength region, and the observed intensity of the 129.6 nm emission line from the $6s'[1/2]_1$ state was much weaker than the 147 nm line (a factor of 100). The reason for the poor response is the three reflective surfaces (the grating and two mirrors) in the optical system of the Minuteman monochromator. The quality and cleanness of the surfaces are very important in the short wavelength region and the optics of this monochromator are 15 years old. The dye laser energy for excitation of Xe($6p'$) atoms (~225 nm) also is weaker than the energy to excite Xe($6p$) atoms (~250 nm). Despite all these problems, averaging ~2000 laser pulses provided wave forms for the decay of the 129.6 nm emission intensity from $6s'[1/2]_1$ atoms of acceptable quality.

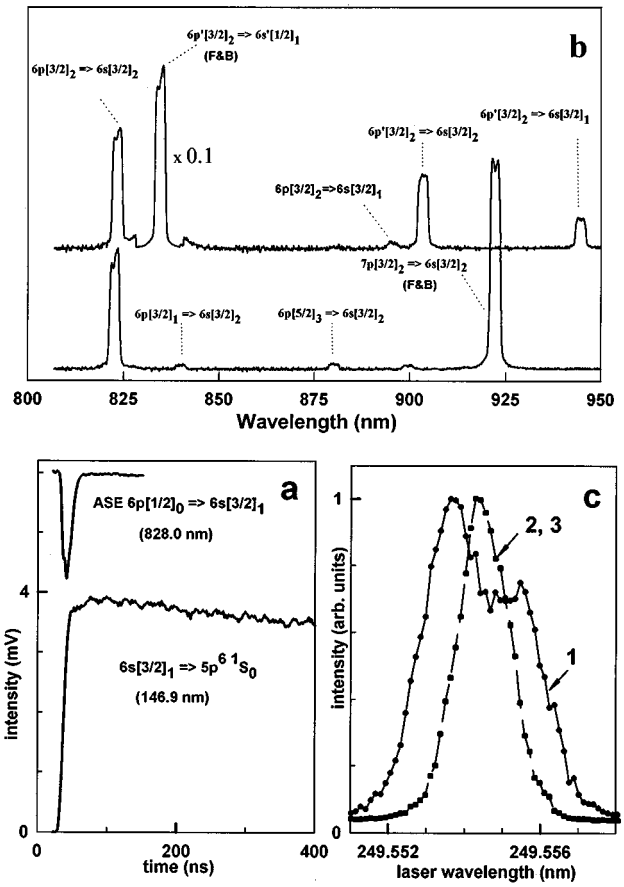

FIG. 3. (a) Wave forms of backward (ASE) emission and the 147 emission for two-photon excitation of Xe($6p[1/2]_0$) for a focused and laser energy of ~0.1 mJ in 1 Torr of Xe. (b) Spectra of forward emission measured with OMA under two-photon excitation of $6p'[3/2]_2$ (top) and $7p[3/2]_2$ (bottom) in 10 Torr of Xe with a laser energy of ~0.25 mJ. Only transitions marked as ''F&B'' also were observed in the backward direction. Spectra are not corrected for the response of the OMA.; the lines for $\lambda > 900$ nm are from the second order. (c) Excitation spectra of forward(1) and backward(2) emissions of the Xe($6p[1/2]_0 \rightarrow 6s[3/2]_1$) transition at 828 nm and the Xe($6s[3/2]_1$) atom concentration (3) measured in the range of $6p[1/2]_0 \rightarrow 5p^6(^1S_0)$ two-photon resonance in 5 Torr for a laser energy of 0.25 mJ. The excitation spectrum for the Xe($6s[3/2]_1$) atoms was obtained via observation of the 147 nm resonance fluorescence in the direction perpendicular to propagation of the laser beam.

III. EXPERIMENTAL RESULTS

ASE and other nonlinear phenomena under two-photon excitation of xenon

The amplified spontaneous emission develops from the inverted population of atoms in the two-photon excited state, relative to lower state(s) that are connected with the upper one via one-photon selection rules, $\Delta J = 0, \pm 1$, and $\Delta 1 = \pm 1$. As a macroscopic effect, the ASE can occur only above certain threshold conditions determined by the natural lifetime, the concentration of the laser-excited atoms, the length of the medium, and other factors; this question has been thoroughly considered in the literature.[13] The important feature for our present purposes is that for conditions well above threshold, the ASE pulse occurs within the time of the laser pulse. A typical wave form of the ASE from the Xe($6p[1/2]_0 \rightarrow 6s[3/2]_1$) transition is shown in Fig. 3(a) (the temporal behavior of the 147 nm fluorescence is discussed in the next section). The second important feature is that the intensity of the ASE depends only very weakly on the presence of foreign gases, primarily because of the very short effective lifetime of atoms involved in the process of stimulated emission. Study of the $6p'[3/2]_2 \rightarrow 6s'[1/2]_1$ ASE transition in a few Torr of Xe and a laser energy of ~0.1 mJ showed that addition of up to 20 Torr of gases such as CH_4, N_2O, and SF_6 had little effect on the ASE intensity, although the quenching rate constants of the $6p'[3/2]_2$ atoms by these gases are $2-4\times10^{-9}$ cm^3/s.[12] According to our estimate, the effective lifetime of the $6p'[3/2]_2$ atoms is ~0.5 ns or less for experimental conditions well above the ASE threshold.

ASE is not the only nonlinear optical phenomena that could occur under two-photon excitation of the Xe($6p$,$6p'$) states.[14] Off-resonant excitation could give stimulated electronic Raman scattering (SERS). Since SERS follows the same selection rules as ASE and also has bidirectional gain, this process cannot be distinguished from resonantly produced ASE, if the tuning range of SERS is smaller then our laser bandwidth. The off-resonant SERS photons could participate in additional nonlinear interactions. Figure 3(b) presents a spectrum of forward emission measured under two-photon excitation of $6p'$ and $7p$ states. The appearance of the Xe($6p-6s$) lines, as assumed in early studies,[12,14(a)] is due to ASE cascade processes involving $5d$ or $7s$ levels

acting as intermediate states. However, we found none of the $6p \rightarrow 6s$ lines in the backward emission spectra. Since ASE has bidirectional gain, this result suggests that some of these lines may have a Raman nature. An especially interesting case arises when the lower state of the SERS process is radiatively coupled with the ground state of the atom, because the mixing of SERS and laser emissions could result in coherent emission to the ground state. This process, which requires the same phase-matching conditions between the pump and self-generated waves as four-wave mixing, $2k_L = k_1 + k_2$, can have gain only in the forward direction (in the general case at a certain angle to the pump beam). Such types of processes have been observed in alkali-metal vapors and atomic oxygen.[15] Our experiments with two-photon excitation to the $6p[1/2]_0$ state showed that the intensity of the $6p[1/2]_0 - 6s[3/2]_1$ emission (828 nm) in the forward and backward directions displays different dependencies on laser power, xenon pressure and—what is most striking—the excitation spectra of the forward and backward emissions are different too. The excitation spectrum of the backward emission [see Fig. 3(c)] has the same shape as the excitation spectrum of the Xe($6s[3/2]_1$) atom concentration, as measured by the 147 nm sideband fluorescence, while the spectrum of the forward emission is broader. This result implies that the $6p[3/2]_0 \rightarrow 6s[3/2]_1$ forward emission being excited in the wings of the excitation spectrum does not create population in the $6s[3/2]_1$ state, but presumably results in development of coherent emission to the ground state of atom. In fact, we were able to observe this emission in the range of $6s[3/2]_1 \rightarrow 5p^6(^1S_0)$ resonance transition by directing the laser beam to the cell through an additional entrance window situated in the front of the LiF window (see Fig. 2). The temporal behavior of the observed signal was similar to that of the $6p[3/2]_0 \rightarrow 6s[3/2]_1$ forward emission. A more detailed description of the generation of the coherent 147 nm emission will be published separately[16] (see also the Discussion Section of the present paper). Our present interest is the resonant ASE, which transfers an actual Xe atomic concentration from the $6p[1/2]_0$ laser excited state to the Xe($6s[3/2]_1$) resonance state.

Generation of Xe($6s[3/2]_1$) atoms by two-photon excitation of Xe($6p[1/2]_0$)

Two-photon-excitation of $6p[1/2]_0$ at 249.6 nm was found to be the preferred method for the generation of $6s[3/2]_1$ resonance atoms. Most experiments were performed with a mildly focused laser beam in a few Torr of Xe. For these conditions the rise time of the 147 nm fluorescence signal is within the ASE pulse [see Fig. 3(a)]. The correlation of the 147 nm fluorescence intensity vs the ASE intensity for different xenon pressure and laser energies is shown in Fig. 4. As expected, this correlation is linear, since the ASE emission is responsible for generation of the $6s[3/2]_1$ atoms. After termination of the ASE pulse, the 147 nm fluorescence exhibits single exponential decay; see Fig. 5(a). For Xe pressures of a few Torr and laser energy ~0.1 mJ, the intensity of the 147 nm signal was quite strong (~100 photons per laser pulse) and only ~100 laser shots were needed to obtain a high quality wave form. A set of wave forms for mixtures with N_2 is shown in Fig. 6, as an example of the quenching data. Adding a few Torr of N_2 decreases the decay

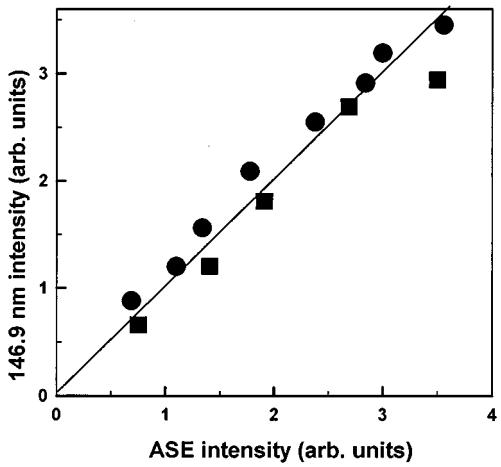

FIG. 4. Intensity of 147 resonance fluorescence vs intensity of ASE ($6p[1/2]_0 \rightarrow 6s[3/2]_1$ transition). The data (■) were taken by varying the laser energy from 0.08–0.2 mJ with 3 Torr of Xe. The data (●) were taken for 1–8 Torr Xe pressure at constant laser energy of 0.15 mJ.

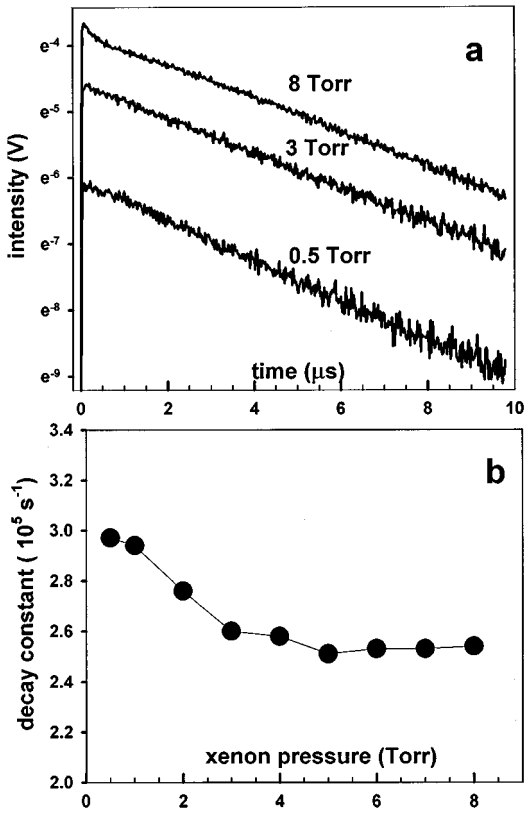

FIG. 5. Dependence of the decay of 147 nm intensity (log scale) on Xe pressure. (a) Wave forms of the 147 nm resonance fluorescence for different Xe pressures. (b) Decay constants of the 147 nm fluorescence vs Xe pressure.

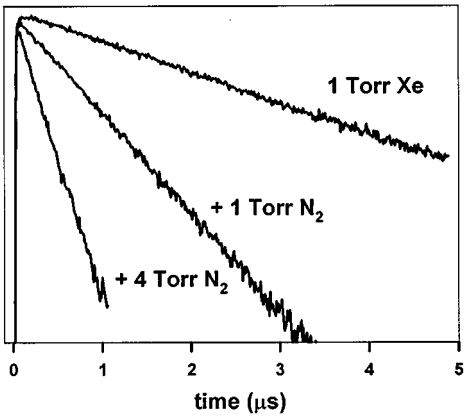

FIG. 6. Wave forms of 147 nm fluorescence intensity (log scale) used to measure the quenching rate constant by N_2. The Xe pressure was 1 Torr and the focused laser energy was 0.1 mJ.

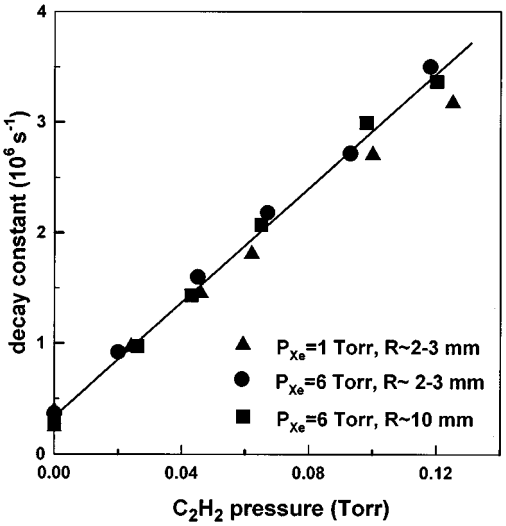

FIG. 7. Plot of decay rate constants for 147 nm emission vs C_2H_2 pressure. The decay constants were measured for two different distances between the laser beam and LiF window and two different Xe pressures. The decay rate of the trapped radiation for $R \approx 10$ mm is ~1.5 times slower than that for $R \sim 2$–3 mm; however, the difference is not evident on the scale of the plot.

time of the 147 nm fluorescence, but the N_2 does not affect the peak intensity of the signal, i.e., the $6s[3/2]_1$ formation step.

Although the natural radiative lifetime of $6s[3/2]_1$ atoms is 3.5–4.5 ns,[17] the effective lifetime of the resonance radiation in pure Xe is lengthened greatly due to radiation trapping. The effective lifetime, τ_{eff}, depends on Xe pressure and other experimental factors, such as the distance (R) between the observation window and the laser beam (i.e., the volume containing the excited atoms) and the cell dimensions. For Xe pressures of 1–10 Torr and a distance of 2–3 mm, τ_{eff} was a few μs. In this pressure range, the decay rate of the 147 nm emission depends only weakly on xenon pressure [Fig. 5(b)]. The Holstein theory[18] for the transport of resonance radiation predicts a region in which the exponential decay rate is independent of pressure with a decay constant given by Eq. (1)

$$\beta_0 = \frac{0.269}{\tau_0}\left(\frac{\lambda}{R}\right)^{1/2}, \tag{1}$$

where R is the radius of the cylinder, τ_0 is the natural lifetime of the transition having wavelength λ. Equation (1) gives $\beta_0 \sim 0.5$–1.0×10^6 s^{-1} for $R \sim 3$ mm, which is in acceptable agreement with our data [Fig. 5(b)].

The geometrical arrangement of the cell affects the decay time for resonance radiation. In particular, if the diffusion of resonance radiation affects the field of view, the decay may be nonexponential.[11] We always observed single exponential decay in our experiments, if the laser beam was in front of the entrance slit of the monochromator. The explanation is that after radiation reached the observation window, the concentration of excited atoms in each element of volume can be factored, as shown in Eq. (2), into a radial dependence and a time dependence.

$$N(r,t) = f(r)\exp(-\beta t). \tag{2}$$

The decay constant, β, includes all processes in the observed volume that deplete the excited atoms. When a reagent is added, $\beta = \beta_0 + k_Q[Q]$, where the first term is determined by Eq. (1) for our pressure range. For more details about the radiation imprisonment problem, see Ref. 11 and references therein.

We did not study the temporal behavior of the 147 nm emission for different alignments of laser beam relative to the entrance slit in any detail. However, the independence of the quenching rate constant measurements on geometric factors and Xe pressure was verified. Data for acetylene are shown in Fig. 7 for two different distances between the laser beam and the observation window and two Xe pressures. Within the experimental uncertainties, the geometric factors and Xe pressure did not affect the quenching rate, although the effective lifetime of trapped radiation did increase with distance. Similar test experiments with other molecules revealed no influence of geometric factors or Xe pressure on quenching rate constants.

Quenching constants for Xe($6s[3/2]_1$) atoms

Quenching rate constants of the first Xe resonance state atoms were measured for 11 molecules at a constant Xe pressure of 1.0 Torr and laser energy of ~0.1 mJ. At least two independent sets of wave forms were measured for each molecule to obtain the rate constant. A set of wave forms was already shown in Fig. 6 to illustrate the first-order decay of the Xe($6s[3/2]_1$) atom concentration in N_2. Single exponential decay exists over two decades of $6s[3/2]_1$ concentration. However, care must be exercized because the decay rates can change by an order of magnitude as the reagent is added. We experienced some difficulty with the band pass of a preamplifier, and the wave forms were acquired without a preamplifier. Also, one must guard against distortion of the wave forms from afterpulses of the PMT. The Stern–Volmer plots for several molecules are shown in Figs. 8(a) and 8(b); the other data are of similar quality. The reagent pressure usually

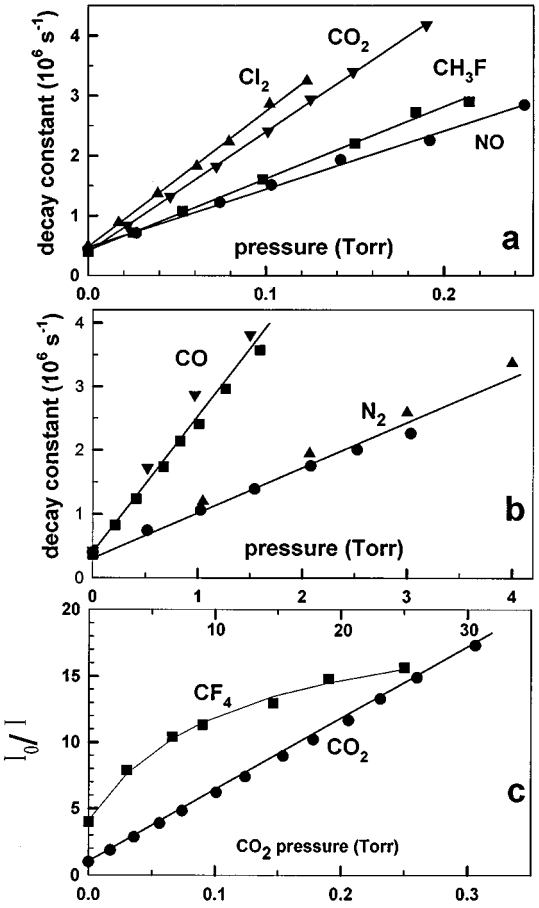

FIG. 8. (a) Decay constants of 147 nm fluorescence vs pressure of Cl_2, CO_2, CH_3F, and NO. The decay constants were measured with $P_{Xe}=1$ Torr for a focused laser energy of ~0.1 mJ. (b) Decay constants of 147 nm fluorescence vs CO and N_2 pressure. Two independent sets of data are shown for each molecule. The Xe pressure was 1 Torr and the laser energy was ~0.1 mJ. (c) Plot of the ratio of the integrated intensity of the 147 nm fluorescence without reagent vs the intensity with reagent. The Xe pressure was 1 Torr and the laser energy was ~0.1 mJ. The scale for CF_4 pressure is shown at the top of the plot; the I_0/I values for CF_4 have been multiplied by four for convenience of presentation; thus, the zero CF_4 pressure value actually is the same as for the CO_2 plot. See Discussion section of text for a description of the wave forms for CF_4.

was increased until the decay constants increased by a factor of 8–10. Except for CO and N_2, the quenching rates are very fast, and <0.5 Torr of the reagent was needed to establish the Stern–Volmer plot. The addition and measurement of the small partial pressures of the reagents could be a limiting factor to the reliability of the rate constants. The data were taken by first adding Xe to the cell and subsequently adding the reagent from a reservoir via a needle value. A wave form was taken for each reagent pressure. The increase in pressure was measured by a pressure transducer placed directly on the cell. The 300 K rate constants are listed in Table I. The typical reproducibility in k_Q values for different data sets was ±5%.

The quenching rate constant for CO_2 was also obtained from the decrease of the integrated 147 nm intensity as the CO_2 pressure was increased. The kinetic equation for this case can be obtained by integration of Eq. (3) over r and t.

TABLE I. Total quenching constants[a] for Xe($6s[3/2]_1$) and Xe($6s'[1/2]_1$) atoms.

Molecule	$6s[3/2]_1$ (This work)	$6s[3/2]_2$ (Ref. 1)	$6s'[1/2]_1$ (This work)	$6p[3/2]_2$ (Ref. 26)
N_2	0.19	0.19	3.7	1.9(3.1)[b]
CO	0.63	0.36	3.3	3.6
NO	3.0	2.7	8.0	7.4
CO_2	5.2	4.5	7.6	
N_2O	7.2	4.4	9.8	7.8(8.2)
CH_4	3.3	3.3	10	
CH_3F	3.7	3.3	11	
CCl_4	7.8	6.3	8.1	7.8(7.3)
Cl_2	6.9	7.2	8.0[c]	14.5(13.3)
CIF	7.5	6.0		
C_2H_2	7.5	7.0	12	

[a]In units of 10^{-10} cm^3 s^{-1}; the uncertainties of the rate constants for the $6s[3/2]_1$ and $6s'[1/2]_1$ atoms, are ±5% and ±10%, respectively.
[b]The number in parenthesis is the rate constant for the Xe($6p[5/2]_2$) state.
[c]The uncertainty for this rate constant is ±20% because of experimental difficulties with a photomultiplier tube and with passivation of the cell.

$$I = C/(\beta_0 + k_Q[Q]). \tag{3}$$

The constant, C, depends upon geometry and other experimental factors. The ratio of the integrated intensity without and with added reagent is given by Eq. (4).

$$I_0/I = 1 + \beta_0 k_Q[Q]. \tag{4}$$

The data gave the expected linear plot for a broad range of CO_2 pressure [Fig. 8(c)]. For the calculation of k_Q, we used the β_0 value measured in the real time experiments. Within 15% uncertainty, the integrated intensity data gave the same value for k_Q as the real time experiment (see Table I).

The set of relative rate constants measured by Yu[8(b)] for $6s[3/2]_1$ atoms are the only data available for comparison. The rate constant with CO_2, which was the molecule used as a reference by Yu, was measured several times for different geometries and the reproducibility was ±5%. The relative values of our rate constants are summarized in Table II and the agreement with Yu's results is satisfactory for molecules

TABLE II. Relative quenching rate constants of the Xe($6s[3/2]_1$) and Xe($6s[3/2]_2$) atoms and summary of optical absorption cross-sections.

	Relative quenching rate constants[a]			σ_{abs} (10^{-18} cm^2)[b]	
Molecule	$6s[3/2]_1$ (This work)	$6s[3/2]_1$ [Ref. 8(b)]	$6s[3/2]_2$ (Ref. 1)	146.9 nm	129.6 nm
N_2	0.04	0.035	0.04	0.02	0.02
CO	0.12	0.21	0.09	0.02	0.02
NO	0.58	0.76	0.60	0.2	2
CO_2	1.00	1.00	1.00	0.7	0.8
N_2O	1.38	1.69	0.98	8.7	97
CH_4	0.63	0.85	0.73	0.02	20
CH_3F	0.71	0.86	0.98	0.4	12
CCl_4	1.5	3.5[c]	1.4	16	64
Cl_2	1.33	1.39	1.6		
C_2H_2	1.44	3.5[c]	1.56	81	36

[a]Relative to the rate constant for CO_2.
[b]Adapted from Refs. 27 and 28.
[c]These values are too large, presumably because absorption of the 147 nm radiation affected the data of Ref. 8(b).

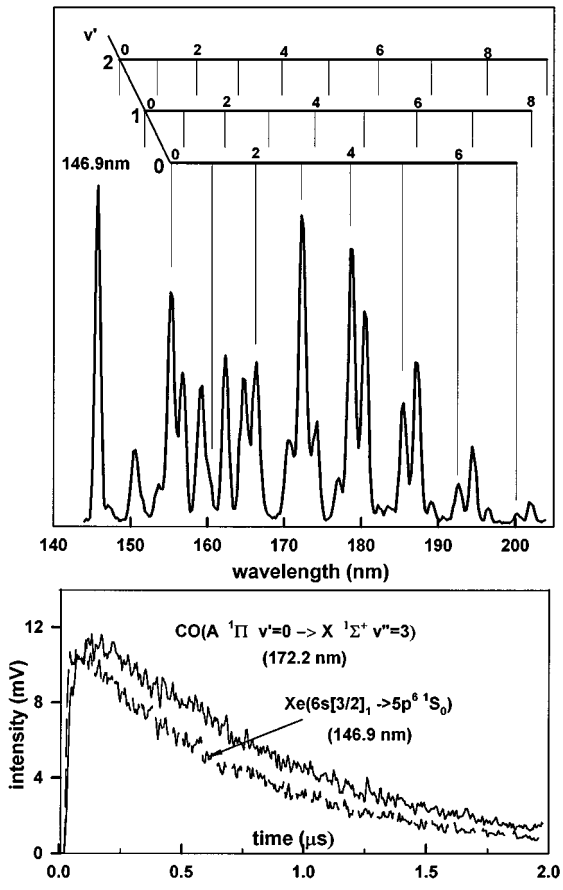

FIG. 9. The CO($A^1\Pi - X^1\Sigma^+$) emission spectrum and the Xe($6s[3/2]_1$) and CO($A^1\Pi$) decay profiles. The Xe and CO pressures were 1 Torr and the laser energy was ~0.1 mJ.

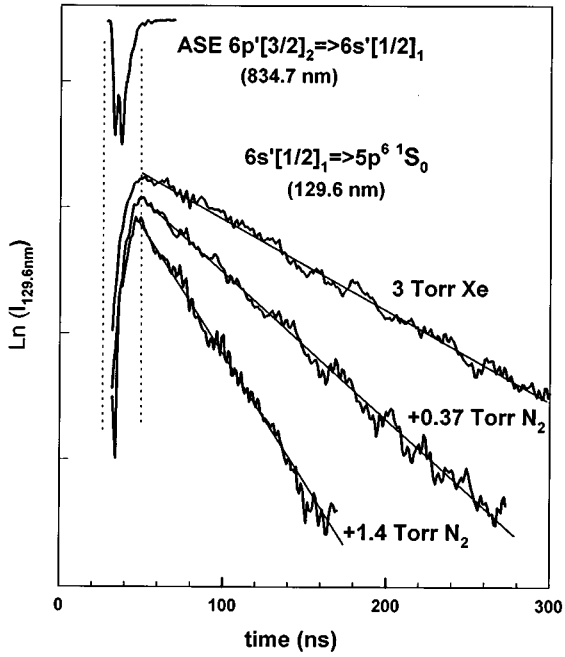

FIG. 10. Wave forms of the 129.6 nm resonance fluorescence intensity (log scale) from Xe($6s'[1/2]_1$) atoms obtained under two-photon excitation of Xe($6p'[3/2]_2$). The Xe pressure was 3 Torr and laser energy was ~0.2 mJ. A wave form of the ASE (8347 nm) for the same experimental conditions (observed in the backward direction) is shown for comparison.

that do not strongly absorb 147 nm light, even though the experimental methods were quite different. Our value for k_{CO_2} can be used to place Yu's relative rate constant values on an absolute basis.

The reaction of $6s[3/2]_1$ atoms with CO gave strong CO ($A^1\Pi$, $v'=0,1-X^1\Sigma^+$) emission in the 150–190 nm range; (see Fig. 9). This result is in agreement with Slanger,[19] who reported excitation transfer to CO($A^1\Pi, d^3\Delta, e^3\Sigma, a'^3\Sigma^+$). The lifetime for CO($A^1\Pi$) is 10 ns[20] and quenching and relaxation is not important; however, collisional transfer into CO($A^1\Pi$) from the longer lived CO(d,e,a') molecules does occur. This may explain the presence of CO($A^1\Pi$, $v'=0$), which is 2,320 cm^{-1} below the $6s[3/2]_1$ energy. The most important aspect of Fig. 9 is the time dependence of the CO($A-X$) emission, which rises quickly and then decays with the same decay constant as Xe($6s[3/2]_1$) atoms. This observation effectively nullifies the claim by previous workers[19] that the quenching mechanism proceeds by a Xe·CO* long-lived, bound intermediate. The CO reaction will be examined further in the Discussion section. The products from $6s[3/2]_1$ atoms with RX (X=halogen) already have been studied using the steady-state sensitization method and synchrotron excitation;[8] the branching fractions for XeX* formation seem to be similar to those for reactions of $6s[3/2]_2$ metastable atoms. No systematic attempt was made in the present work to study products from the reactions of $6s[3/2]_1$ atoms. Such studies would be especially interesting for CO and N_2. The ASE method can be used at Xe pressures of ~0.1 Torr (we did observe ASE in this pressure range) and the major difficulty to systematic observation of products is the required pressure of CO (N_2) needed to obtain measurable product fluorescence intensities. However, the fluorescence could be observed for short times using gating techniques to reduce the effects of collisional relaxation.

Generation of Xe($6s'[1/2]_1$) atoms by two-photon excitation of the $6p'[3/2]_2$ state

Two-photon excitation of the $6p'[3/2]_2$ state was used for generation of the second Xe resonance state atoms. The $6p'[3/2]_2 \rightarrow 6s'[1/2]_1$ transition (834.7 nm) has a branching fraction[21,22] of 0.73, and the ASE was easily observed for mildly focused conditions. The $6p'[1/2]_0 \rightarrow 6s'[1/2]_1$ (788.7 nm) transition, which also could be used to generate $6s'[1/2]_1$ atoms, has a branching fraction of 0.62.[21,22] Since neither of these $6s'$ states are radiatively coupled with the $6s'[1/2]_0$ metastable atoms, generation of the $6s'$ metastable atoms is not a complication. The two-photon cross section for excitation of $6p'[1/2]_0$ is 20% bigger than that for $6p'[3/2]_2$,[12] but excitation of $6p'[1/2]_0$ requires 222.5 nm and the BBO-I crystal has poor efficiency at this wavelength. Due to this reason and also the better branching fraction, the $6p'[3/2]_2$ state was used in our experiments. A typical set of wave forms for decay of the $6s'[1/2]_1 \rightarrow 5p^6(^1S_0)$ emission at 129.6 nm is shown in Fig. 10. Due to the poor response of

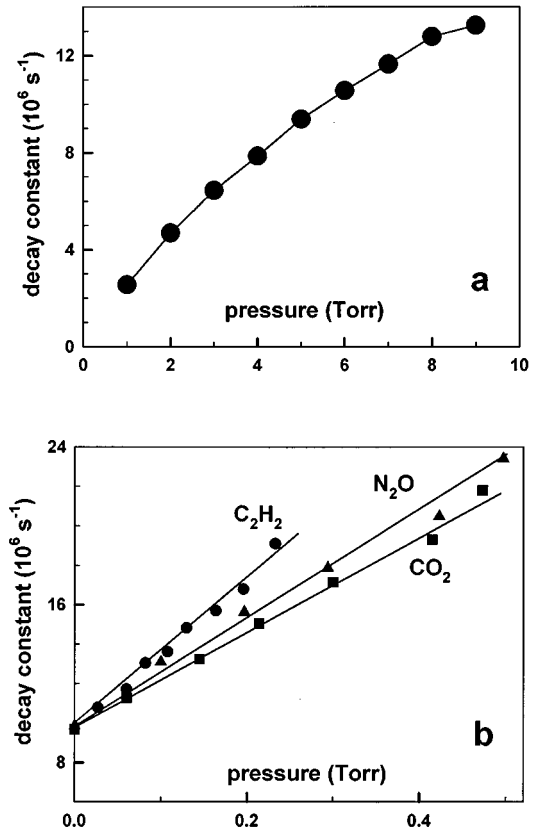

FIG. 11. Stern–Volmer plots of first-order decay constants of Xe($6s'[1/2]_1$) atoms vs pressure. (a) Decay constants of 129.6 nm fluorescence vs Xe pressure. (b) Decay constants of the 129.6 nm fluorescence vs C_2H_2, N_2O, and CO_2 pressure from experiments with 3 Torr of Xe and a laser energy of 0.2 mJ.

our registration system, the intensity of the 129.6 nm emission was 100 times lower than of the 147 nm emission for comparable intensities of the $6p[1/2]_0 \rightarrow 6s[3/2]_1$ and $6p'[3/2]_2 \rightarrow 6s'[1/2]_1$ ASE transitions (i.e., for comparable concentrations of the $6s[3/2]_1$ and $6s'[1/2]_1$ atoms).

The $6s[3/2]_1$ and $6s'[1/2]_1$ atom concentrations have greatly different decay times and dependence of decay times on xenon pressure [compare Figs. 5(b) and 11(a)]. The $6s'[1/2]_1$ atoms are collisionally coupled with the close-lying $6p[1/2]_1$ atoms ($\Delta E = 84$ cm^{-1}); the latter radiatively decay to the Xe($6s$) states with a radiative lifetime of ~35 ns.[9(d),22] The 300 K rate constant for reaction (5),

$$\mathrm{Xe}(6s'[1/2]_1) + \mathrm{Xe} \rightarrow \mathrm{Xe}(6p[1/2]_1) + \mathrm{Xe}, \tag{5}$$

was reported as $(6.6 \pm 1.0) \times 10^{-11}$ cm^3/s by Sadeghi and Sabbagh.[23] More recent measurements of Alford[9] favor an even larger value $(10.1 \pm 4.5) \times 10^{-11}$ cm^3/s and $(6.7 \pm 4) \times 10^{-11}$ cm^3/s for the reverse process. For high enough xenon pressure, the reverse transfer from $6p[1/2]_1$ would couple the concentrations in the two states, and they would have an effective radiative lifetime of ~100 ns. At 3 Torr, the reverse transfer rate is only 1/4 of the radiative rate from $6p[1/2]_1$. As a consequence, the decay of $6s'[1/2]_1$ at 3 Torr of Xe is determined mainly by process (5), which should have a rate of $\sim 9 \times 10^6$ cm^3/s, and this value is in acceptable agreement with our experiment, 6.5×10^6 cm^3/s [Fig. 11(a)]. The $6s'[1/2]_1$ decay rate, as monitored by the 129.6 nm emission, has a tendency to saturate [see Fig. 11(a)] at higher Xe pressure, because of the collisional coupling between the $6s'[1/2]_1$ and $6p[1/2]_1$ states. Our data certainly support a large rate constant for process (5). However, experiments with simultaneous observation of the 129.6 nm emission and the $6p[1/2]_1 \rightarrow 6s[3/2]_2$ infrared emission (980 nm) could provide better data. Other questions of interest are the collisional relaxation rates from the $6s'[1/2]_1$ and $6p[1/2]_1$ levels to $6s'[1/2]_0$ and the Xe($6s$) product states. The rate constants currently assigned to these processes from various studies[9] are somewhat in disagreement, because of indirect monitoring of the products.

The question of formation of $6s[3/2]_1$ atoms during two-photon pumping of the $6p'[3/2]_2$ state needs separate consideration. Even below the threshold for ASE, the mechanism of this process is complicated and can involve both collisional relaxation via different intermediate states and spontaneous radiative decay

$$\begin{aligned} &\mathrm{Xe}(6p'[3/2]_2) + \mathrm{Xe} \rightarrow \mathrm{Xe}^{**} + \mathrm{Xe} \\ &\mathrm{Xe}^{**} + \mathrm{Xe} \rightarrow \mathrm{Xe}(6s[3/2]_1) + \mathrm{Xe} \\ &\mathrm{Xe}^{**} \rightarrow \mathrm{Xe}(6s[3/2]_1) + h\nu. \end{aligned} \tag{6}$$

The collisional relaxation of $6p'[3/2]_2$ atom in Xe was studied by Keto and co-workers[24] and by ourselves.[12] Although state-to-state rate constants were not assigned, collisional relaxation ultimately feeds the Xe($6s$) levels, which was confirmed in the present work by observation of 147 nm emission for unfocused two-photon excitation of the $6p'[3/2]_2$ state (i.e., below the ASE threshold). Excitation above the threshold for the $6p'[3/2]_2 \rightarrow 6s'[1/2]_1$ ASE transition changes the processes that produce the $6s[3/2]_1$ state population. Some of the wave forms for the 147 nm emission observed when pumping $6p'[3/2]_2$ had rise times in the same time domain as the decay of the 129.6 nm emission, which suggests that collisional transfer from $6s'[1/2]_1$ to $6p[1/2]_1$ followed by radiative decay to the $6s[3/2]_1$ state is the major formation pathway. However, the fast rise of the 147 nm signal within the laser pulse was observed in some cases too. Presumably direct and cascade transitions, $6p'[3/2]_2 \rightarrow 6s[3/2]_1$ (473.4 nm) and $6p[3/2]_2 \rightarrow 6s[3/2]_1$ (895.1 nm), see Fig. 3(b), are responsible for feeding the $6s[3/2]_1$ state during the laser pulse. In general, the temporal behavior of 147 nm emission under excitation of the $6p'[3/2]_2$ state seems to be very sensitive to experimental conditions (laser energy, spatial and temporal coherence of the laser beam etc.), which were difficult to control in our experiments. Detailed consideration of the mechanisms for formation of Xe($6s[3/2]_1$) resonance atoms when pumping Xe($6p'$ or $7p$) states is beyond the scope of present work. The two-photon excitation of the $6p[1/2]_0$ state clearly is much more desirable for preparation of Xe($6s[3/2]_1$) atoms than two-photon excitation of the $6p'[3/2]_2$ state.

Quenching rate constants for Xe($6s'[1/2]_1$) atoms

These experiments were done using two-photon excitation of $6p'[3/2]_2$ in 3 Torr of Xe for the generation of $6s'[1/2]_1$ resonance atoms; quenching rate constants were measured for the same molecules (except ClF) as for the $6s[3/2]_1$ atoms. The wave forms for the decay of the 129.6 nm emission intensity were strictly single exponential, but due to the low response of our registration system at 130 nm, the quality of the data were not so high as for the 147 nm data. A typical set of wave forms used to establish a quenching rate constant is shown in Fig. 10 and Stern–Volmer plots for several molecules are shown in Fig. 11(b). The quenching rate constants are listed in Table I. Due to the weaker emission intensities, the uncertainty in these rate constants are two times larger than for Xe($6s[3/2]_1$) atoms. All the rate constants for Xe($6s'[1/2]_1$) atoms are larger than those for Xe($6s[3/2]_1$) atoms; however, the rate constants for Cl_2 and CCl_4 are only slightly larger than for the $6s[3/2]_2$ metastable or $6s[3/2]_1$ resonance atoms. To the best of our knowledge, no other data for Xe($6s'[1/2]_1$) atoms are available for comparison.

Quenching rate constants for Xe($6s'[1/2]_0$) metastable atoms also are not available. The $6s'[1/2]_0$ atoms are collisionally deactivated in He, and the lifetime of the $6s'[1/2]_0$ atoms were too short for quenching rate constant measurements in a discharge flow reactor.[25] However, product distributions from reactions of $6s'[1/2]_0$ atoms with some reagents have been made.[25] Since comparison cannot be made with metastable $6s'[1/2]_0$ atoms, quenching rate constants for Xe($6p[5/2]_2$ and $[3/2]_2$) states[26] are included in Table I; these states are only 0.12 and 0.25 eV above the $6s'[1/2]_1$ state. In general, the magnitudes of the rate constants for Xe($6s'[1/2]_1$) and Xe($6p$) atoms seem to be comparable.

Attempts to identify products from reaction of $6s'[1/2]_1$ atoms were not very successful. Difficulties arose because of the collisional transfer of atoms from the $6s'[1/2]_1$ level to the $6p[1/2]_1$ state (see above), which then radiatively decays to Xe($6s$) atoms, and also the generation of Xe($6s$) atoms by ASE cascade and/or Raman processes. In principle, differences in energy and effective lifetimes of Xe($6s'$) and Xe($6s$) atoms could be used to identify the products from their respective reactions. For example, we observed that the reaction of Xe($6s'[1/2]_1$) atoms with CF_3I gave I($6s^2P_{3/2}$) and I($6s^4P_{3/2}$) atoms, whereas these excited atomic iodine states are energetically forbidden from reactions with Xe($6s$) atoms.

IV. DISCUSSION

Two-photon driven ASE from XE($6p$) and Xe($6p'$) states as a time-resolved method for generating Xe resonance state atoms

The utilization of ASE for detection of atoms in flames[29] and for molecular spectroscopy[30] has attracted attention in recent years. Our experiments have demonstrated that two-photon resonance excitation of Xe($6p$ and $6p'$) atoms followed by ASE is a simple and effective method for the generation of Xe resonance state atoms on a 20 ns time frame. The method could be used for other atomic systems as outlined below. Presumably, the time scale could be shortened by using a laser with a shorter pulse. The method is suitable for accurate measurement of total quenching constants, because the formation of Xe($6s$ or $6s'$) atoms occurs during the laser pulse and because the reagent concentration is not seriously affected by the laser pulse. The method is less desirable for observation of nascent product states that are relaxed or quenched by collisions with the reagent gas. However, the method should be applicable to study the two- and three-body decay kinetics of Xe($6s[3/2]_1$) and Xe($6s'[1/2]_1$) atoms in rare gases with observation of dimer emission. Coupling observation of the decay of the 147 and 129.6 nm fluorescence with probing of the Xe($6s[3/2]_2$) atom concentration by absorption spectroscopy can give a complete view of the kinetics of these states. The time-revolved emission from the XeRg* dimers could be observed to provide elucidation about the three-body processes. In such work, care must be exercised to allow for changes in the effective radiative decay rate induced by the high pressure of added reagent gas.

The ASE and Raman phenomena occurring under two-photon excitation of xenon are themselves of fundamental interest. The generation of intense, coherent (vac. UV) emission due to four-wave mixing (FWM) observed in this work will be considered in detail in the future.[16] Although the lack of wavelength tunability is an obvious limitation, this effect could be a source of pulsed vac. UV light for photochemical studies. Measurement of the energy and the conversion efficiency for this FWM beam are needed. Preliminary results suggest that the two-photon excitation of $6p'[3/2]_2$ state also could generate coherent vac. UV emission in the vicinity of the $6s'[1/2]_1 \rightarrow 5p^6(^1S_0)$ transition at 129 nm.[16] Another aspect of interest is the possible competition between FWM and ASE, which could result in partial suppression of the latter. Such a process was observed for two-photon excitation of the Na($3d$) level in sodium vapor.[15(b)] The nature of the suppression is the destructive interference between two pathways of excitation for the two-photon resonance state, $\omega_L+\omega_L$ and $\omega_1+\omega_2$ where ω_1 and ω_2 are self-generated waves. This interference reduces the concentration of two-photon pumped atoms and, consequently, the ASE.[15(c)] The same effect presumably could occur in our experiments. The fact that the excitation spectrum of the forward emission (the sum of FWM and ASE) has a minimum at the wavelength where the excitation spectrum of backward emission (only ASE) has a maximum suggests a higher intensity of FWM than ASE. This question is related to optimization of the ASE method for generating resonance states and needs more detailed study. The FWM can be minimized by choice of experimental parameters such as the length of the cell and the confocal parameter of the laser beam.[15] In any event, the work here demonstrates that any decrease of the ASE generation of resonance atoms due to FWM is not a serious restriction.

The upper limit to the Xe($6s[3/2]_1$) and Xe($6s'[1/2]_1$) atom concentrations is defined by the onset of plasma formation that is generated by multiphoton ionization during the

laser pulse or afterwards by bimolecular collisional ionization of the Xe($6s$ and $6s'$) atoms. The formation of excited Xe($6p$,$6p'$) states on a μs time scale via collisional processes from Xe($6s$) atoms was confirmed in the present work.[26] Observation of emission from the Xe($6p$,$6p'$) states for times >100 ns after the laser pulse provides a convenient diagnostic test for the onset of plasma formation. If the Xe($6p[3/2]_2$) state is selected for two-photon excitation rather than $6p[3/2]_0$, then a large component of the ASE branching is to the metastable Xe($6s[3/2]_2$) state, and the subsequent generation of excited states of Xe by collisional ionization seems to occur more readily than for two-photon excitation via the $6p[1/2]_0$ state, which generates only Xe($6s[3/2]_1$) resonance atoms. The greater tendency for collisional ionization for experiments that generate metastable Xe($6s[3/2]_2$) atoms may reflect a higher concentration of the metastable atoms than the resonance state atoms or possibly different ionization rate constants. At any rate, the experimental conditions specified for this work provide a time-resolved source of resonance state atoms that is free of slow formation steps that could affect study of the decay kinetics of the $6s[3/2]_1$ and $6s'[1/2]_1$ atoms.

The two-photon driven ASE method can be applied to the selective generation of resonance states of other atoms that normally require one-photon excitation in the vac. UV. It is promising, in particular, for the first resonance state of Kr. Excitation to the Kr($5p$) levels requires two 215 nm photons, which can be obtained using a BBO-II crystal. In fact, ASE from the Kr($5p\rightarrow 5s$) transitions already has been observed,[14(a)] and Kr($5s[3/2]_1$) resonance atoms definitely can be studied by the two-photon driven ASE method. Two-photon excitation of Xe($7p$) states offers an interesting possibility for generating of the $5d[1/2]_1$ (125.02 nm) and $7s[3/2]_1$ (117.04 nm) resonance states of Xe. Transitions from the Xe($7p$) levels to these resonance states have significant branching ratios ($\sim$0.2).[21] In particular, the branching ratios and probabilities for the ($7p[1/2]_0\rightarrow 5d[1/2]_1$, $7s[3/2]_1$) transitions in the infrared (1128.9, 2939.2 nm, respectively) and the $7p[1/2]_0\rightarrow 6s[3/2]_1$) visible transition (480.7 nm) are nearly the same. Since the ASE at 480.7 was observed (see Fig. 2), one could expect the ($7p\rightarrow 5d$,$7s$) ASE transitions too. However, radiative coupling of the $5d[1/2]_1$ and $7s[3/2]_1$ states with the $6p$ states could result in serious depletion of the concentrations. We would not have observed emission from Xe($5d[1/2]_1$) and Xe($7s[3/2]_1$) states in the present work, even if it existed, because our detection system has little or no response at 125 and 117 nm). The kinetics of $5d[1/2]_1$ and $7s[3/2]_1$ states have never been studied in detail, except for some very recent work of Castex and co-workers,[31] who used four-wave mixing in mercury vapor to obtain the necessary vac. UV emission in the range of the $5d[1/2]_1\leftarrow 5p^6(^1S_0)$ transition. The $5d[1/2]_1$ state is the second level in the $5d$ manifold about which little information is known, and finding an improved way to study the $5d[1/2]_1$ state would represent an important advance for characterization of the excited states of Xe.

Quenching rate constants the Xe($6s[3/2]_1$) and Xe($6s'[1/2]_1$) atoms

When discussing quenching of the metastable states of rare gas atoms, it is customary to divide the reagents into two classes based upon the magnitude of their cross-sections.[1(b)] The smaller group has cross-sections less than 20 Å^2 and includes molecules with a low density of excited states, such as CO and N_2, which quench by interaction of the entrance channel with specific exit channel potentials.[32] The larger group, which includes nearly all polyatomic molecules except CF_4, have large quenching cross-sections, because of the large probability, P, of energy transfer for those collisions with an impact parameter smaller than the orbiting distance, i.e., $\sigma_R = P\pi b_0^2$. These two categories seem useful for the resonance states too, although the resonance and metastable atoms could have a different physical basis for quenching, even if P is of similar magnitude. For atoms or molecules with no excited acceptor states in the 8.4 or 9.6 eV range, the rate constant for the resonance atoms can be larger due to collisional relaxation to the lower energy metastable state. In addition, such atoms or molecules could influence the effective decay rate of trapped radiation due to the collisional broadening of the resonance line. The photoabsorption spectra of Rg/CF_4 mixtures (Rg=Xe,Kr) show strong blue-wing broadening of the $(n+1)s[3/2]_1\leftarrow np^6(^1S_0)$ resonance line together with the appearance of a blue satellite at $P_{CF_4} \geqslant 1$ atm.[33] Collisional line broadening increases the decay rate of the trapped radiation, but it does not affect the total integrated emission intensity. Experiments with CF_4 during the course of the present work did illustrate this phenomena. The addition of CF_4 resulted in a faster decay rate of the 147 nm emission **and** an increase in the 147 nm peak intensity (adding $\sim$3 Torr of CF_4 to a 1 Torr Xe sample gave a two-fold enhancement of the peak 147 nm signal). Furthermore, the observed decay of the 147 nm intensity was not single exponential. The nonsingle exponential nature is presumably due to the collisional coupling of the resonance and metastable atoms. Golde[34] already has suggested that collisions of CF_4 with $6s[3/2]_2$ atoms transfer population to the $6s[3/2]_1$ level. A plot of the integrated 147 nm intensity vs CF_4 pressure [see Fig. 8(c)] was used to estimate the rate constant for quenching the $[3/2]_1$ atoms to the $[3/2]_2$ metastable state. The estimated value is $3\text{–}6\times 10^{-12}$ cm^3 s^{-1}, which is consistent with the quenching constant for Xe($[3/2]_2$).[1(b)] Such a strong influence of collisional broadening on the decay rate of the trapped radiation seems specific for CF_4; no evidence of this effect was found for other molecules used in the present work. The explanation probably is the much smaller quenching cross-section for CF_4. Collisional line broadening and the effect upon the effective radiative decay time of the resonance state atoms must be remembered for reagents with small quenching constants.

The present work allows the quenching rate constants for the metastable Xe($6s[3/2]_2$) and resonance state Xe($6s[3/2]_1$) atoms to be compared, see Table I. Since the data for the metastable and resonance states were obtained with quite different experimental methods, systematic ex-

perimental error could be involved in either or both sets of experiments and measurement of both constants in the same experiment would be desirable. Nevertheless, several of the rate constants for the metastable atoms have been measured more than one time, and the reliability should be ±20%, and we believe that the rate constants for $6s[3/2]_1$ atoms obtained in this work are very reliable. Except for CO and N_2O, all molecules have nearly the same quenching rate constant for both $6s$ states, which differ in energy by 0.12 eV. From the viewpoint of the orbiting model, the quenching cross-sections of the Xe($6s$) pair are expected to be the similar, although interplay of such factors as symmetry and energy resonances could influence the values of p. The excitation-transfer mechanism with identification of a small number of product states is well documented for $6s[3/2]_2$ atoms interacting with CO and N_2.[32] Our current work together with Slanger's early studies[19] demonstrate a similar mechanism for quenching $6s[3/2]_1$ atoms by CO. The similar rate constants for Cl_2 and CCl_4 for the Xe($6s$) and Xe($6s'$) atoms suggest the dominance of reactive quenching. The $6s'[1/2]_1$ and $6p[3/2]_2$ or $6p[5/2]_2$ states differ in energy by 0.12 and 0.25 eV, respectively, and their cross-sections invite comparison. Since the polarizabilities and sizes of $6p$ atoms are larger than $6s$ atoms, the orbiting cross sections also are larger. As shown in Table I, the rate constants for Xe($6s'[1/2]_1$) atoms are larger than for the Xe($6s'[3/2]_1$) atoms and more similarity exists between the Xe($6p$) and Xe($6s'$) atoms that for Xe($6's$) and Xe($6s$) atoms. This similarity arises, in part, because of extensive configurational mixing of the Xe($6s'$) states with the Xe($5d$) states.[35]

Along with collisional quenching, the more trivial mechanism of photoemission by Xe* followed by absorption of the photon by the molecule needs to be considered. This absorption would not seriously influence the decay rate of the resonance emission, if the probability of molecular photoabsorption during the lifetime of the trapped radiation is small. A criteria for the neglect of such absorption can be formulated as $\sigma_{Xe}[Xe]/\sigma_Q[Q] \gg \tau_{tr}/\tau$ where τ and τ_{tr} are the natural lifetime of resonance state and the lifetime of trapped radiation for a given [Xe] (and for a given geometry), respectively. The lifetime ratio is the number of emission-absorption acts occurring in pure xenon before a resonance photon escapes the cell, and this number is $\sim 10^3$ for our experimental conditions. The cross-section term is the ratio of optical depths of the atomic and molecular components of the mixture; for one emission-absorption cycle this ratio equals to the ratio of probabilities of photon absorption by Xe or by the reagent. The absorption cross-section[27] at the center of the 147 nm line is 2.9 10^{-12} cm^{-2}, which is 10^5 larger than typical absorption cross sections of the molecules (Table II). Since the typical [Xe]/[Q] ratio is ~10 in our experiments, molecular absorption does not influence the decay rate of the trapped radiation.

In some cases analysis of the emission spectra of products can distinguish between collisional excitation-transfer reactions and dipole–dipole coupling, the latter has the same selection rules as photoabsorption. In particular, Slanger observed prominent differences in the CO* fluorescence spectra obtained with Xe-resonance lamp excitation of pure CO vs sensitization of CO+Xe mixtures.[19] The dipole–dipole quenching cross-section[10] is given by Eq. 7.

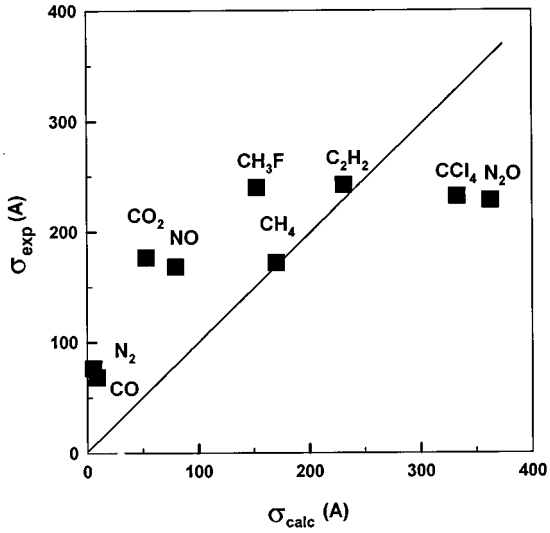

FIG. 12. Plot of the experimental quenching cross-sections of ($6s'[1/2]_1$) atoms vs calculated cross-section using the Watanabe–Katsuura formula (Ref. 10).

$$\sigma_Q = 13.88(\mu_{Xe}^2 \mu_Q^2 / h\upsilon)^{2/5} \ \{\text{a.u.}^2\}. \quad (7)$$

The μ_{Xe} and μ_Q terms are the dipole transition matrix elements of the Xe resonance and molecular transitions at the wavelength of the atomic transition, respectively and υ is the relative collision velocity. The transition matrix elements are given by the following relation

$$\mu_{Xe}^2 = (R/E) f_{Xe} \quad \text{and} \quad \mu_Q^2 = (2R^2/4\pi^2 \alpha a_0^2 E)\sigma_{abs}, \quad (8)$$

where R, α, a_0, E, f_{Xe}, and σ are the Rydberg constant, the fine structure constant, the Bohr radius, the energy of resonance state, the oscillator strength of the resonance transition, and the photoabsorption cross-section, respectively. The average experimental thermal cross-sections $(k(T)/\langle\upsilon\rangle)$ for Xe($6s'[1/2]_1$) atoms are compared to those calculated from the Watanabe–Katsuura formula in Fig. 12. The value of f_{Xe} for the 129.6 nm line, 0.306, was taken from Ref. 21; the molecular absorption cross-sections were taken from Refs. 27 and 28. A positive correlation between the experimental and calculated cross-sections does exist, although the agreement between absolute values is poor, except for CH_4 and C_2H_2. The latter could be accidental because $\sigma_{abs}(C_2H_2)$ is larger at 147 than 129.6 nm, whereas $k_Q(6s[3/2]_1) < k_Q(6s'[1/2]_1)$. Furthermore, the rate constants for CH_4 with the $6s[3/2]_1$ and $6s[3/2]_2$ atoms are similar, but $\sigma_{abs}(CH_4)$ changes by an order of magnitude. The set of rate constants for quenching of $6s'[1/2]_1$ atoms obtained in the present work is too limited to confirm or refute the applicability of the dipole–dipole model. The data for Xe($6s[3/2]_1$) atoms are not shown in Fig. 12, because few of the molecules in Table II have large absorption cross-section at 147 nm; however, the relatively large rate constants in Table I and Ref. 8(b), show that the dipole–dipole mecha-

nism must not be the only quenching process. The existing data for $Xe(6s)$ and $Xe(6s')$ resonance atoms do not provide strong support for a dipole–dipole mechanism. This is in contrast to the claim for quenching of $Ar(4s[3/2]_1$ and $4s'[1/2]_1)$ atoms by SF_6, CH_4, SiH_4, and GeH_4.[6(b),6(c)] The choice of a set of reagent molecules plays a key role in any definitive test, because the dipole–dipole cross-section has to be larger than the curve-crossing contribution to the cross-section. This requirement excludes molecules with large electron affinities, such as halides and oxides. Furthermore, the set must be sufficiently large to avoid giving undue weight to cases that fortuitously suggest agreement with the theory. The best selection of molecules to test the dipole–dipole model are those with small polarizability, small electron affinities, and moderate to large absorption cross-section. Some relatively simple hydrocarbons can satisfy these requirements. Acquiring such a comprehensive set of rate constant data was beyond the scope of the present investigation, although the two-photon driven ASE method can yield such data for $Xe(6s[3/2]_1$ and $6s'[1/2]_1)$ atoms.

V. CONCLUSIONS

Two-photon driven amplified spontaneous emission from $Xe(6p[1/2]_0)$ and $Xe(6p'[3/2]_2)$ states provides excellent time-resolved sources for the $Xe(6s[3/2]_1)$ and $Xe(6s'[1/2]_1)$ resonance state atoms, respectively. The method was demonstrated by measuring the quenching rate constants for 10 reagent molecules at 300 K using 1–3 Torr of Xe and 0.3–3 Torr of reagent. These rate constants were compared to those for $Xe(6s[3/2]_2)$ metastable atoms and $Xe(6p)$ atoms. The rapid rise of the $CO(A^1\Pi)$ emission from the excitation-transfer reaction between CO and $Xe(6s[3/2]_1)$ atoms shows that this quenching process does not involve a long-lived, bound Xe·CO intermediate. Providing that care is exercised in selection of materials for the photolysis cell, the ASE method can be extended to low and high temperature measurements. In addition to the amplified stimulated emission, the single-color, two-photon excitation of the $Xe(6p, 6p'$ and $7p)$ states in low pressure of Xe can produce other nonlinear Raman scattering processes, and these also may have practical importance. Three-photon resonance ionization[36] and collisional ionization processes also can occur and care must be exercised in choosing experimental conditions to control the degree of ionization.

ACKNOWLEDGMENTS

This work was supported by the U.S. National Science Foundation Grant CHE-9402012. We thank Dr. Nader Sadeghi, Joseph Fourier University, Grenoble III for the loan of a photomultiplier tube, which allowed this work to be completed.

[1] (a) J. E. Velazco, J. H. Kolts, and D. W. Setser, J. Chem. Phys. **69**, 4357 (1978); **71**, 1247 (1978); (b) X. Chen and D. W. Setser, J. Phys. Chem. **95**, 8473 (1991); (c) D. Zhong, D. W. Setser, R. Sobczynski, and W. Gadomski, J. Chem. Phys. (in press); (d) N. Sadeghi, M. Cheaib, and D. W. Setser, J. Chem. Phys. **90**, 219 (1989).

[2] (a) J. Balamuta, M. F. Golde, and Y-S. Ho, J. Chem. Phys. **79**, 2822 (1983); (b) J. Balamuta and M. F. Golde, *ibid*. **76**, 2430 (1982); (c) J. Balamuta, M. F. Golde, and A. M. Moyle, *ibid*. **82**, 3169 (1985); (d) M. F. Golde and Y-S. Ho, *ibid*. **82**, 3160 (1985).

[3] (a) K. Tamagake, J. H. Kolts, and D. W. Setser, J. Chem. Phys. **71**, 1264 (1979); (b) K. Johnson, R. Pease, J. P. Simons, P. A. Smith, and A. Kvaran, J. Chem. Soc. Faraday Trans. 2. **82**, 1281 (1986); (c) M. S. de Vries, G. W. Tyndall, C. L. Cobb, and R. L. Martin, J. Chem. Phys. **84**, 3753 (1986).

[4] (a) M. Ukai, Y. Tanaka, H. Koizumi, K. Shinsaka, and Y. Hatano, J. Chem. Phys. **84**, 5575 (1986); (b) H. Yoshida, Y. Morishima, M. Ukai, and K. Shinsaka, Chem. Phys. Lett. **176**, 173 (1991).

[5] (a) A. Yokoyama and Y. Hatano, Chem. Phys. **63**, 59 (1981); (b) A. Yokoyama, S. Takao, T. Ueno, and Y. Hatano, *ibid*. **45**, 439 (1980).

[6] (a) References before 1978 are summarized in Ref. 1(a); (b) M. Ukai, H. Koizumi, K. Shinsaka, and Y. Hatano, J. Chem. Phys. **84**, 3199 (1986); (c) H. Yoshida, H. Kawamura, M. Ukai, N. Kouchi, and Y. Hatano, *ibid*. **96**, 4372 (1992).

[7] (a) H. C. Brashers and D. W. Setser J. Phys. Chem. **84**, 224 (1980); (b) H. C. Brashers, D. W. Setser, and Y. C. Yu, *ibid*. **84**, 2495 (1980); J. Chem. Phys. **74**, 10 (1981); (c) Y. C. Yu and D. W. Setser, J. Phys. Chem. **94**, 2934 (1990); (d) Y. C. Yu and K. J. Wang, J. Photochem Photobiol. A: Chem. **72**, 109 (1993).

[8] (a) D. Lin, Y. C. Yu, and D. W. Setser, J. Chem. Phys. **84**, 5830 (1984); (b) Y. C. Yu, J. Photochem Photobiol. A: Chem. **47**, 259 (1989).

[9] (a) W. J. Alford, J. Chem. Phys. **96**, 4330 (1992), and references therein; (b) P. Laporte, J. C. Subtil, R. Reininger, and P. Gürtles, Chem. Phys. **177**, 257 (1993); (c) P. Moutard, P. Laporte, J. C. Subtil, N. Damany, and H. Damany, J. Chem. Phys. **88**, 7485, (1988).

[10] T. Watanabe and K. Katsuura, J. Chem. Phys. **47**, 800 (1967).

[11] (a) C. E. Klots, J. Chem. Phys. **56**, 124 (1972); (b) G. S. Hurst, E. B. Wagner, and M. G. Payne, *ibid*. **61**, 3680 (1974).

[12] V. A. Alekseev and D. W. Setser, J. Phys. Chem. **100**, 5766 (1996).

[13] See L. Allen and G. I. Peters, J. Phys. A **5**, 695 (1972), and references therein.

[14] (a) J. C. Miller Phys. Rev. A. **40**, 6969 (1989); (b) M. B. Rankin, J. P. Davis, C. Giranda, and L. C. Bobb, Opt. Comm. **70**, 345 (1989).

[15] (a) S. M. Hamadani, J. A. D. Stockdale, R. N. Compton, and M. S. Pindzola, Phys. Rev. A **34**, 1938 (1986); (b) M. S. Malcuit, D. J. Gauthier, and R. W. Boyd, Phys. Rev. Lett. **55**, 1086 (1985); (c) R. W. Boyd, M. S. Malcuit, D. J. Gauthier, and K. Rzazewski, Phys. Rev. A **35**, 1648 (1987); (d) M. E. Riley, *ibid*. **41**, 4843 (1990).

[16] V. A. Alekseev and D. W. Setser, Chem. Phys. Lett. (to be published).

[17] E. Matthias, R. A. Rosenberg, E. D. Poliakoff, M. G. Whitte, S.-T. Lee, and D. A. Shirley, Chem. Phys. Lett. **52**, 239 (1977).

[18] T. Holstein, Phys. Rev. **72**, 1212 (1947); *ibid*. **83**, 1159 (1951).

[19] T. G. Slanger and G. Black, J. Chem. Phys. **51**, 4534 (1969); *ibid*. **58**, 194, 3121 (1973); *ibid*. **59**, 4367 (1973).

[20] A. LeFloch, J. Rostas, and F. Rostas, Chem. Phys. **142**, 261 (1990).

[21] M. Aymar and M. Coulomb, Atomic Data, and Nuclear Data Tables, **21**, 538 (1978).

[22] H. Horiguchi, R. F. S. Chang, and D. W. Setser, J. Chem. Phys. **73**, 1207 (1981).

[23] N. Sadeghi and J. Sabbagh, Phys. Rev. A **16**, 2336 (1977).

[24] C. A. Whitehead, H. Pournasr, M. R. Bruce, H. Cai, J. Kohel, W. B. Layne, and J. Keto, J. Chem. Phys. **102**, 1965 (1995).

[25] D. Zhong and D. W. Setser, Chem. Phys. Lett. **207**, 555 (1993).

[26] T. O. Nelson, D. W. Setser, and M. K. Richman, J. Chem. Phys. **99**, 7482 (1995).

[27] H. Okabe, *Photochemistry of Small Molecules* (Wiley, New York, 1978).

[28] M. Robin *High Excited States of Molecules* (Academic Press, New York, 1974).

[29] (a) R. A. Copeland, J. B. Jeffries, A. P. Hickman, and D. R. Crosley, J. Chem. Phys. **86**, 4876 (1987); (b) M. Alden, U. Westblom, and J. E. M. Goldsmith, Opt. Lett. **14**, 305 (1989); (c) H. Bergstrom, H. Hallstadius, H. Lundberg, and A. Persson, Chem. Phys. Lett. **155**, 27 (1989); (d) V.-L. Huang and R. J. Gordon, J. Chem. Phys. **97**, 6363 (1992).

[30] (a) J. W. Glesser and J. J. Davis, J. App. Phys. **73**, 2672 (1993); (b) J. Ishii, K. Uehere, and K. Tsukiyama, J. Chem. Phys. **104**, 499 (1996).

[31] L. Museur, A. V. Kanaev, W. Q. Zheng, and M. C. Castex, J. Chem. Phys. **101**, 10548 (1995).

[32] (a) Ch. Ottinger, A. F. Vilesov, and D. D. Xu, Chem. Phys. **192**, 49 (1995); (b) T. Krumpelmann and Ch. Ottinger, Chem. Phys. Lett. **140**, 142

(1987); (c) T. G. Aardema, E. J. van Nijnatten, and H. C. W. Beijerinck, Chem. Phys. **184**, 273 (1994).

[33] (a) V. A. Alekseev, N. K. Bibinov, and I. P. Vinogradov, Opt. Spectrosc. **73**, 154 (1992); (b) V. A. Alekseev and I. P. Vinogradov, *ibid*. **76**, 644 (1993).

[34] (a) J. Balamuta, M. F. Golde, and A. M. Moyle, J. Chem. Phys. **82**, 3169 (1985); (b) M. F. Golde and Y.-S. Ho, *ibid*. **82**, 3160 (1985).

[35] (a) S. J. Liberman, J. Phys. **30**, 53 (1969); (b) M. C. Coulombe and J. Sinzelle, *ibid*. **36**, 774 (1975).

[36] A. W. McCown, and M. N. Ediger, and J. G. Eden, Phys. Rev. A **26**, 2281 (1982).